1-13-2011

Room Temperature Ferromagnetism and Optical Limiting in V(2)O(5) Nanoflowers Synthesized by a Novel Method

Manas R. Parida
Indian Institute of Technology - Madras

C. Vijayan
Indian Institute of Technology - Madras

Chandra Sekhar Rout
Purdue University, crout@purdue.edu

C. S. Suchand Sandeep
Raman Res Inst - Bangalore

Reji Phiip
Raman Res Inst - Bangalore

See next page for additional authors

Parida, Manas R.; Vijayan, C.; Rout, Chandra Sekhar; Sandeep, C. S. Suchand; Phiip, Reji; and Deshmukh, P. C., "Room Temperature Ferromagnetism and Optical Limiting in V(2)O(5) Nanoflowers Synthesized by a Novel Method" (2011). *Birck and NCN Publications.* Paper 776.
http://docs.lib.purdue.edu/nanopub/776

Authors
Manas R. Parida, C. Vijayan, Chandra Sekhar Rout, C. S. Suchand Sandeep, Reji Phiip, and P. C. Deshmukh

Room Temperature Ferromagnetism and Optical Limiting in V_2O_5 Nanoflowers Synthesized by a Novel Method

Manas R. Parida,[†] C. Vijayan,*[,†] C. S. Rout,[‡] C. S. Suchand Sandeep,[§] Reji Philip,[§] and P. C. Deshmukh[†]

Department of Physics, Indian Institute of Technology, Madras, Chennai, India, Birck Nanotechnology Center, Purdue University, West Lafayette, Indiana, United States, and Raman Research Institute, Bangalore, India

Received: August 19, 2010; Revised Manuscript Received: October 9, 2010

We report on the observation of room temperature ferromagnetism as well as optical limiting in V_2O_5 nanoflower structures synthesized by a simple and novel cost-effective low-temperature method. The flowers are characterized thoroughly by various analytical techniques to ascertain their structure and composition and to confirm the absence of any impurities. The samples exhibit ferromagnetic properties at 300, 200, and 100 K observed from a hysteresis loop. Coercivity for room temperature synthesized V_2O_5 flowers is 566 Oe at 300 K and is enhanced at 200 and 100 K. We propose a growth mechanism of the flowers and attribute the origin of ferromagnetism to the introduction of oxygen vacancies in accordance with theoretical predictions available on other oxide nanomaterials. The samples also show optical limiting behavior arising from an effective three photon absorption mechanism as demonstrated by a Z-scan experiment for characterization of optical nonlinearity.

1. Introduction

Vanadium pentoxide (V_2O_5) has been in the forefront of applied research in view of its multifunctional properties, which include optical, electronic, reduction/oxidation, and electrochromic properties.[1a] V_2O_5 is the most stable form among all vanadium oxides (V_2O_5, V_2O_3, V_3O_5, VO_2, and VO) as it possesses a unique high oxidation state which renders it useful as an amphoteric oxide and oxidizing agent.[1] Nanostructures of V_2O_5 have drawn a tremendous amount of attention as materials used for fabricating various nanodevices such as field effect transistors (FETs),[2] chemical and biosensors[3] and lithium ion battery,[4] supercapacitors,[5] and waveguides.[6] Also, vanadium oxides have been employed for improved physical properties, which include mechanical properties,[7] surface-enhanced Raman spectroscopy,[8] cathodoluminescence,[9] field emission,[10] spintronics,[11] and nonlinear optical studies.[12] Among these various physical and chemical properties, the electrochemical and photochemical properties of V_2O_5 are the most significant ones from a practical point of view. As a Li^+ intercalation host, V_2O_5 has additional advantages because of its layered structure.[4] In addition, V_2O_5 (Eg = 2.8 eV) is susceptible to photoactivation with wavelength less than 443 nm and has been used as a semiconductor-type photocatalyst for the photo-oxidation of cyclohexane in the liquid phase and photocatalytic degradation of water pollutants.[13] This is significant for the use of V_2O_5 as an effective catalyst for photocatalytic degradation of organic pollutants.

A variety of approaches have been used to prepare nanostructures of V_2O_5 from V^{5+} precursors including thermal evaporation,[6] hydrothermal,[3] surfactant-assisted,[2] and template-based synthesis.[10] All these methods are many step based approaches, which require high temperatures for the synthesis of the desired nanostructures. Here we report on the synthesis of V_2O_5 nanoflowers by a novel and simple low-temperature method (at the temperature 300 K) without using any surfactant or capping agent and propose a possible growth mechanism for the flower structures. This approach for synthesis of flowerlike V_2O_5 nanostructures is efficient, economical, and easy to scale up in industrial production in the absence of reductants and requirement of vacuum conditions.

Ferromagnetism in diluted magnetic semiconductors (DMSs) has recently received a lot of attention for fundamental research and possible applications in spintronics.[14] Though a number of metal oxide-based DMSs have been reported, the origin of ferromagnetism in many cases is still under much debate. There is a controversy as to whether magnetism arises because of some intrinsic contribution from the DMS phase or some secondary phases. Oxygen vacancies may also play an important role for the ferromagnetism in oxide-based DMSs because oxygen vacancies not only modulate the valence of the neighboring atoms but also cause a change of the band structures.[11] In this regard, we investigate the magnetic properties of the V_2O_5 flowerlike nanostructures and report on the first observation of room temperature ferromagnetism.

Optical limiting is a phenomenon that has important photonics applications. Optical limiters are devices that show an induced net decrease in transmittance at higher light fluences. These are very useful for protecting sensitive devices and eyes from laser-induced damage. Optical limiters based on nonlinear absorption mechanisms are very efficient. The nonlinear absorption mechanisms involved in such materials are reverse saturable absorption, multiphoton absorption, and free carrier absorption mechanism. Two-photon absorption in several semiconductors such as ZnO, PbS, CdS, and ZnSe and also in some organic materials[24−29] has been shown to result in strong optical limiting. Here we report, for the first time, on the observation of optical limiting based on an effective three-photon absorption in V_2O_5 nanoflowers.

* To whom correspondence should be addressed. Department of Physics, Indian Institute of Technology, Madras, Chennai, India 600036. E-mail: cvijayan@physics.iitm.ac.in.
[†] Indian Institute of Technology.
[‡] Purdue University.
[§] Raman Research Institute.

10.1021/jp107862n
Published on Web 12/14/2010

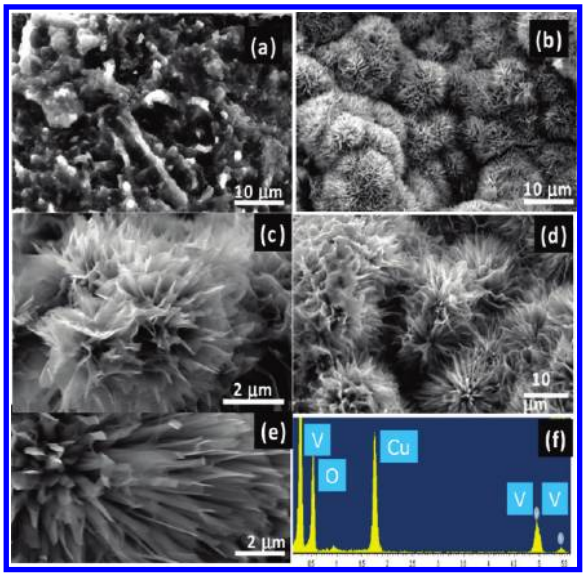

Figure 1. FESEM image of (a) as-prepared vanadium gel, V_2O_5, nanoflowers prepared (b, c) in methanol and (d, e) in ethanol at room temperature; (f) EDAX pattern of the V_2O_5 flowers.

2. Synthesis and Characterization

2.1. Synthesis. In a typical synthesis, 0.5 g of ammonium metavanadate (AMV) (Sigma-Aldrich) is dissolved in 50 mL of deionized water, allowing AMV to completely dissolve under magnetic stirring. Nitric acid is added dropwise to adjust the pH of the solution to ~2 and stirring continued at 323 K. After the water evaporated with stirring, an orange-colored gel of vanadium complex is obtained. The obtained gel is transferred to 20 mL of methanol in a vial and allowed to age for 24 h at room temperature. The color change of the gel from light to dark orange can be observed when it is kept in methanol. After that, the obtained product is washed thoroughly with deionized water before further study. To study the effects of the solvent and temperature on the growth of the flower structure, we followed the same procedure in 20 mL of ethanol and isopropanol at room temperature and at 323 K.

2.2. Results and Discussion. Figure 1a shows the field-emission scanning electron microscopy (FESEM) image of vanadium gel and Figure 1b,c shows representative FESEM images of the V_2O_5 nanoflowers prepared in methanol at room temperature, which confirms the high yield of the flowers. From Figure 1b,c, a flower structure consisting of beltlike petal structures is observed. Figure 1d,e shows FESEM images of the flowers synthesized by treating the gel in ethanol for 24 h at room temperature. On the basis of the FESEM images, the length of the petals prepared in ethanol are larger than the petals of the flower prepared in methanol. Compositions of the flowers were checked by energy-dispersive analysis by X-ray (EDAX). Figure 1f shows an EDAX pattern of the V_2O_5 flowers, which confirms the composition to be only V and O, but the atom ratio of V to O cannot be determined unambiguously since one peak of the element V overlaps the peak of element O. The Cu peak originates from the FESEM grid. Figure 2a,b shows FESEM images of the flowers prepared in isopropanol at room temperature. The obtained flower structures are similar to the as-synthesized flowers in methanol and ethanol. On the basis of the FESEM images (Figure 2c,d), it is clear that the flowers synthesized in methanol at 323 K consist of bundles of nanobelts whose lengths are larger compared to the flower structures at room temperature. FESEM images of the flowers synthesized in ethanol and propanol at 323 K are shown in parts (e) and (f), respectively, of Figure 2.

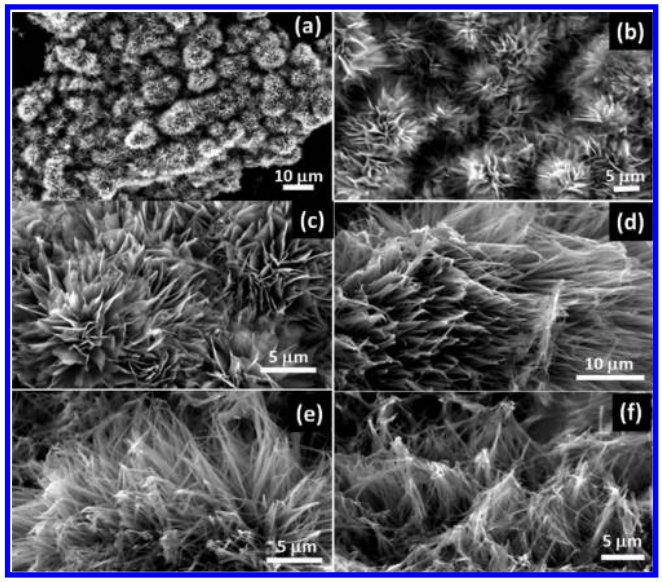

Figure 2. FESEM image of V_2O_5 nanoflowers (a,b) prepared in propanol at room temperature, (c,d) in methanol, (e) in ethanol, and (f) in propanol at 323 K.

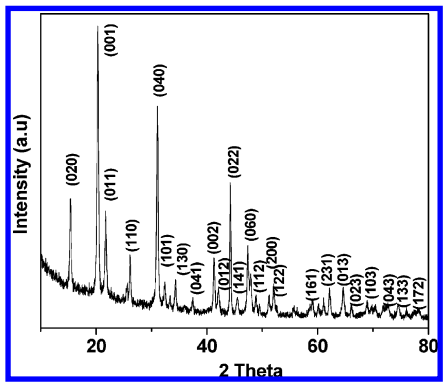

Figure 3. XRD pattern of the V_2O_5 nanoflowers.

Figure 3 shows the typical X-ray diffraction (XRD) pattern of the V_2O_5 flowers prepared at 323 K in ethanol and similar XRD patterns were obtained for all other samples synthesized at room temperature and at 323 K. The XRD patterns of the flower structures can be indexed to the orthorhombic structure of V_2O_5 and are in agreement with the literature values [JCPDS no: 85-0601, lattice parameters: $a = 11.56$ Å, $b = 3.56$ Å, $c = 4.37$ Å]. V_2O_5 nanostructures are believed to be a layered structure in which VO_5 square pyramids are connected by sharing corners and edges.[3] In particular, it is known that this structure permits H_2O molecules to be embedded between the intercalation layers without a far-reaching restructuring, leading to the formation of the $V_2O_5 \cdot xH_2O$ phase.

The as-synthesized flowers are characterized by X-ray photoelectron spectroscopy (XPS) as shown in Figure 4. No peaks of impurity elements are observed in the survey spectrum (Figure 4a). The binding energy obtained in our XPS analysis is corrected for specimen changing by referencing the C(1s) line to 284.5 ev. It is found that the binding energies of the vanadium peaks are centered at 517.04 eV and at 524.47 eV (Figure 4b), which are characteristic of the V^{+5} oxidation state, confirming the formation of V_2O_5. The O(1s) peak at 529.94 eV is attributed to the V−O stretch in V_2O_5 and these values are in agreement with the reported literature.[15]

Figure 5a,b shows TEM images of the petals of the V_2O_5 flowers synthesized in ethanol at 323 K. The diameters of the

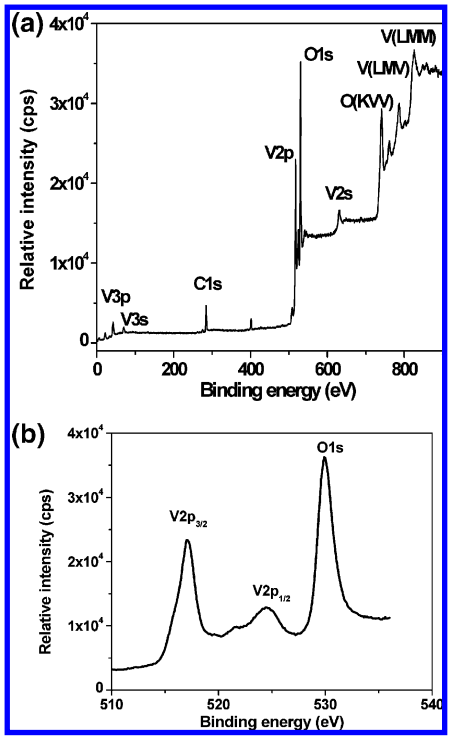

Figure 4. XPS spectra of the as-prepared V_2O_5 nanoflowers prepared in ethanol at 323 K: (a) Wide scan spectrum and (b) high-resolution scan for O(1s) and V(2p).

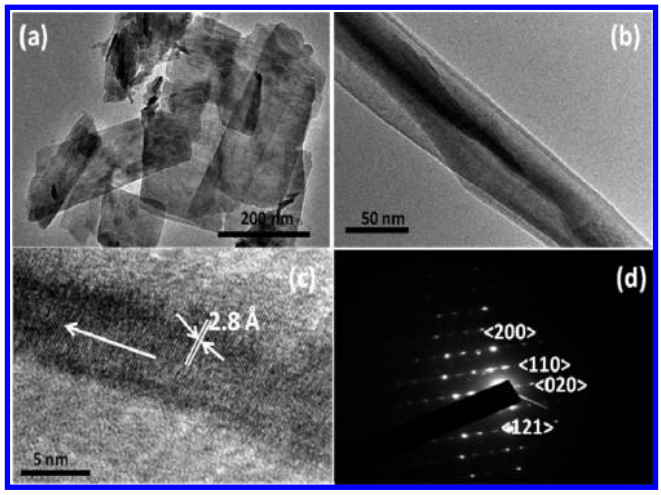

Figure 5. TEM image of (a) petals of the flowers, (b) a single petal, (c) HRTEM image of the petal, and (d) SAED pattern of the petal.

petals are ∼50−200 nm, with a thickness of ∼10−20 nm and length varying up to several nanometers. The petals are very thin, which is clearly observed from the TEM image (Figure 5a). Figure 5c shows a HRTEM image taken from a petal structure. The distance between neighboring planes is ∼2.8 Å, which are consistent with (040) planes of orthorhombic V_2O_5. Corresponding selected area electron diffraction (SAED) pattern is shown in Figure 5d. The SAED pattern indicates the well-crystallized character of the nanoflowers.

Raman spectra of V_2O_5 nanobelts are shown in Figure 6 and acquired Raman peaks match the orthorhombic V_2O_5.[16,17] The low wavenumber peaks at 142 and 193 cm^{-1} correspond to external VO_5-VO_5 modes and indicate the retention of long-range order in nanobelts[16] Peaks at 993 and 696 cm^{-1} correspond to the stretching modes of the V═O (terminal oxygen) and V_2-O (doubly coordinated oxygen) bands, respectively. The peak at 526 cm^{-1} is assigned to the V_3-O (triply coordinated

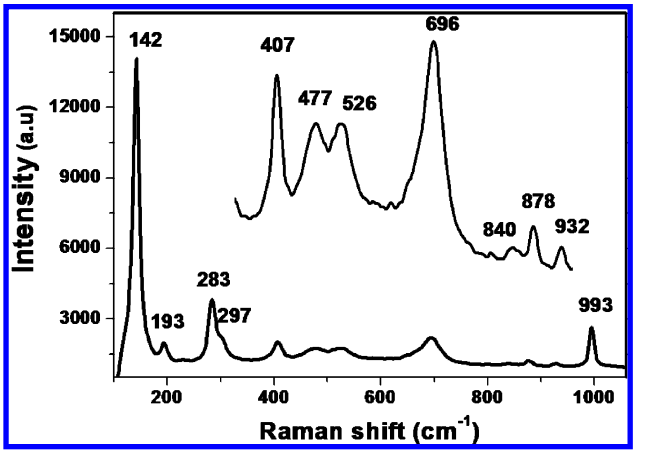

Figure 6. Raman spectra of the as-prepared V_2O_5 nanoflowers.

SCHEME 1: Proposed Growth Mechanism of V_2O_5 Nanoflowers

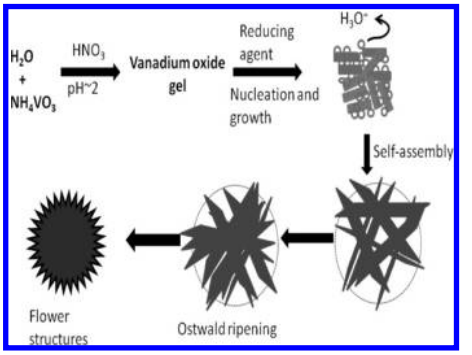

oxygen) stretching mode. Bands at 407 and 283 cm^{-1} are assigned to the bending vibration of the V═O bonds. Band at 477 cm^{-1} can be assigned to the bending vibrations of V−O−V (bridging doubly coordinated oxygen).[16,17]

2.3. Proposed Growth Mechanism. Vanadium oxides are typical intercalation compounds as a result of its layered structures. The intercalation refers to the reversible intercalation of mobile guest species (atoms, molecules, or ions) into a crystalline host lattice that contains an interconnected system of an empty lattice site of appropriate size, while the structural integrity of the host lattice is formally conserved.[1] Since no templates were used in the growth of the nanostructures in the present work, a hydrating, exfoliating-splitting model can be proposed to elucidate the formation of the nanobelts, which is shown in Scheme 1.[1,18] In the formation process, it is believed that V_2O_5 forms a layered structure under the process of hydrolysis and condensation of NH_4VO_3 in the presence of different reducing solvents. The H_3O^+ intercalating and splitting processes determine the formation of the 1D nanostructure in which the added HNO_3 determines the formation of the petals of the flowers. At the initial stage a $[VO(OH)_3]$ unit formed as a result of the protonation of ammonium metavanadate in the presence of HNO_3. Then these $[VO(OH)_3]$ units, each coordinated with two water molecules, were condensed and polymerized to form the layered frameworks of $V_2O_5 \cdot xH_2O$ structures. The interlayer spaces in the layered structures of $V_2O_5 \cdot xH_2O$ are occupied by H_3O^+ ions and thus the interactions between the layers are weakened and the layered $V_2O_5 \cdot xH_2O$ gradually splits to form V_2O_5 petals. The flowers' structures would have formed as a result of the Ostwald ripening and self-assembly of the petals in the presence of methanol, ethanol, and propanol.

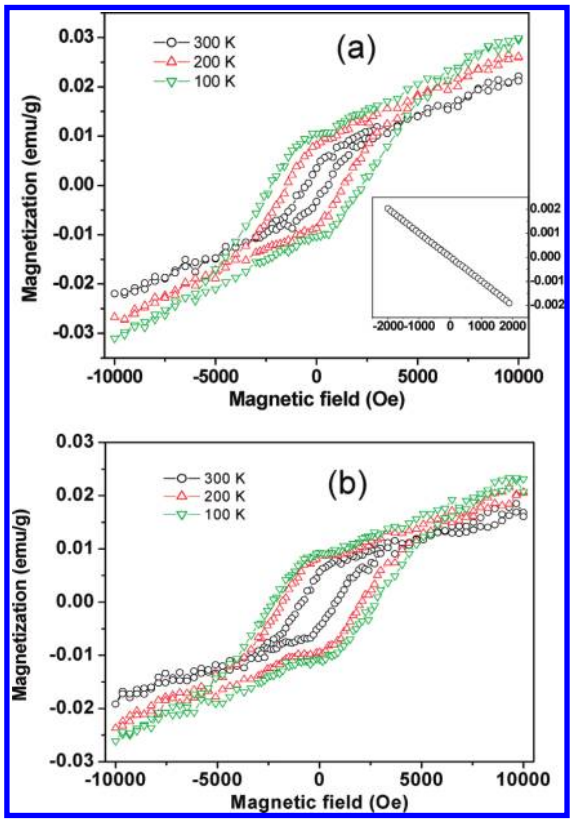

Figure 7. Magnetic hysteresis curves of V_2O_5 flowers at 100, 200, and 300 K synthesized at (a) room temperature and (b) 323 K.

2.4. Room Temperature Ferromagnetism. Parts (a) and (b) of Figure 7 show the magnetization versus magnetic field ($M-H$) curves of the V_2O_5 flowers synthesized in ethanol at room temperature and at 323 K, respectively. The figures show clear hysteresis loops, indicating that V_2O_5 flowers possess room temperature ferromagnetism. This is surprising since bulk V_2O_5 is a high band gap diamagnetic semiconductor with vanadium existing in the V^{5+} valence state.[19] The inset in Figure 7a shows the $M-H$ curve for the sample holder, which is diamagnetic. The coercivity for the room temperature-synthesized V_2O_5 flowers is 566 Oe at 300 K and it is observed that coercivity is enhanced further at 200 and 100 K. The coercivity values (878, 1896, and 2480 Oe at 300, 200, and 100 K, respectively) for this sample are larger compared to those for the room temperature-synthesized flowers. The observed magnetization for our flower samples is much larger compared to the magnetization reported for the Li- and I-doped VO_x nanotubes at room temperature.[11]

Since the XPS studies confirm the absence of any impurity present in our samples, ferromagnetism observed in the present case is not likely to be due to the unintentional doping. Zhang et al. observed that the ferromagnetism of ZnO nanoparticles increases after annealing in vacuum conditions and decreases after annealing in a rich oxygen atmosphere. So it is reported that the oxygen vacancies play an important role in introducing ferromagnetism in the case of ZnO nanoparticles. The origin of magnetism in these V_2O_5 flowers seems to be similar to that reported for other metal oxide nanoparticles, such as those of TiO_2, In_2O_3, and CeO_2 where the oxygen deficiency plays a crucial role. Chen et al. also explained the origin of ferromagnetism in the nanostructure ZnO−Al system is most likely due to the charge transfer between Zn and Al at the interfaces of the ball-milled nanograins.[18] Ferromagnetism in V_2O_5 films has theoretically been related to mechanisms involving oxygen vacancies.[21,22] The vacancies can not only modulate the valence of neighboring elements but also cause a change of the band structure of the host oxides; both factors can make significant contribution to the ferromagnetism. Xiao et al. performed theoretical ab initio studies of the electronic structure and magnetism in V_2O_{5-x}, which can be used to understand the origin of ferromagnetism in the case of V_2O_5 nanoflowers.[21] According to their prediction, the presence of oxygen vacancies introduces electrons onto the neighboring V d_{xy} dominant conduction band, which is then spin-split as a result of intra-atomic exchange interaction, leading to magnetic order. The calculations showed that most of the magnetization is located on the V atoms (d_{xy} orbital) next to the oxygen vacancy and also in the surrounding interstitial region. When one oxygen vacancy is introduced, the lowest conduction band is strongly spin-polarized, and the spin-up one is particularly occupied while the spin-down one is still empty, resulting in a ferromagnetic state with a spin moment of 2 μ_B per vacancy. Clearly, when one oxygen atom is removed, the two electrons released are added to the narrow V d_{xy} dominant conduction band. Hence, the two valence electrons released by the introduction of each oxygen vacancy would occupy mostly the d_{xy} orbital of the V atoms next to the vacancy and become fully spin-polarized as a result of intra-atomic exchange interaction, giving rise to the ferromagnetic order with a magnetic moment of 2 μ_B per vacancy.

We suggest that the unpaired electron spins responsible for ferromagnetism in the nanobelts have their origin in the oxygen vacancies, especially on the surfaces of the oxides. Though the nature of exchange interactions between them is not very clear at present, one may expect that the F centers (electrons trapped in oxygen vacancies) are polarized to give room temperature ferromagnetism. This mechanism has been proposed to explain ferromagnetism in some other transparent oxides.[20] The presence of a larger number of oxygen vacancies in the case of flowers synthesized at room temperature leads to higher magnetization compared to the flowers synthesized at 323 K.

2.5. Nonlinear Optical Response. The samples are found to exhibit large optical nonlinearity, leading to optical limiting behavior. Optical limiting can be due to a variety of nonlinear optical processes such as reverse saturable absorption, multiphoton absorption, and thermal scattering. Optical limiters based on nonlinear absorption mechanisms are known to be very efficient.[23] In the present work, we investigate the absorptive nonlinearity of the nanoflower samples by performing open aperture Z-scan measurements at 532 nm using laser pulses of 5 ns pulse duration. z-scans are single-beam experiments, where the pumping and probing of the medium are done by the same laser pulse. Therefore, the observation of an optical nonlinearity when excited by 5 ns laser pulses indicates that the nonlinearity has a fast component, with an onset time less than 5 ns. The linear transmittance of the sample used for the measurement is 50% at the excitation wavelength.

In our experiment linearly polarized nanosecond laser pulses of approximately 75 μJ pulse energy having a Gaussian beam cross section are used to excite the sample. The beam is focused by a lens, and the sample is moved in fine steps in the vicinity of the focal point ($z = 0$) using an automated translation stage. The sample transmission at each position (z) is measured using a pyroelectric detector. A graph plotted between z and transmittance gives the Z-scan curve (Figure 8a), which in the present case indicates a strong nonlinear absorption. We find that the

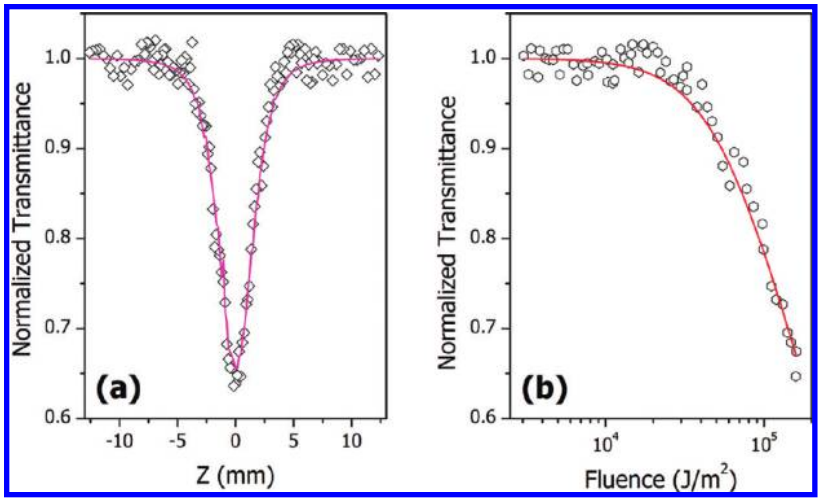

Figure 8. (a) Z-scan curve for V_2O_5 nanoflower; (b) optical limiting of V_2O_5 nanoflower.

data fits best to a three-photon type absorption process, given by the expression[30]

$$T = \frac{(1 - R)^2 \exp(-\alpha L)}{\sqrt{\pi} p_0} \int_{-\infty}^{+\infty} \ln\left[\sqrt{1 + p_0^2 \exp(-2t^2)} + p_0 \exp(-t^2)\right] \mathrm{d}t \quad (1)$$

where T is the transmission of the sample, R is the Fresnel reflection coefficient at the sample−air interface, α is the linear absorption coefficient, and L is the sample length. p_0 is given by $[2\gamma(1 - R)^2 I_0^2 L_{\mathrm{eff}}]^{1/2}$, where γ is the three-photon absorption coefficient and I_0 is the incident intensity. L_{eff} is given by $[1 - \exp(-2\alpha L)]/2\alpha$. The value of the three-photon absorption coefficient γ obtained from the theoretical fit of the Z-scan data is 1.2×10^{-22} m^3/W^2. This value is comparable with that observed in other nanostructure systems such as Se/As_2S_3, Bi-doped ZnO nanoparticles.[31]

Figure 8a indicates rather strong nonlinear absorption with the data fitting very well with the model involving three-photon absorption. The shape of the curve also excludes any contribution from saturable absorption effects. There are only a few earlier reports on nonlinear optical response of vanadium oxide nanostructures. Czerw and co-workers have observed strong optical limiting in vanadium oxide nanotubes and proposed two-photon absorption or excited-state absorption as the predominant mechanism, though they have not attempted fitting to theoretical curves or obtaining the values of the nonlinear parameters.[12a] Hashimoto and Yoko have reported large optical nonlinear coefficients in thin films of vanadium and certain oxides and explained their results based on the values of metal oxide bond lengths in these systems.[12b] Their results are only on refractive nonlinearity measured in thin films using third-harmonic generation, a technique which cannot provide information about nonlinear absorption. In the present work, nonlinear absorption in vanadium oxide nanoflowers is investigated for the first time, leading to the estimation of the nonlinear absorption coefficient by fitting the data from the open Z-scan to a theoretical model based on three-photon absorption.

The optical limiting curve (the plot of normalized transmittance as a function of input laser fluence) is shown in Figure 8b. The incident input laser fluence is given by $4(\ln 2)^{1/2} E_{\mathrm{in}}/\pi^{3/2}\omega(z)^2$ where E_{in} is the input laser pulse energy. $\omega(z)$ is the beam radius and can be expressed as $\omega(0)/[1 + (z/z_0)^2]^{1/2}$ where $\omega(0)$ is the beam radius at focus and $z_0 = \pi\omega^2(0)/\lambda$ is the Raleigh range. The ouput energy is proportional to the input energy for values of input energy less than 2×10^4 J/m^2 and the output energy drops steadily at larger values of input energy. Considering the fact that the sample is semitransparent at the excitation wavelength, the observed nonlinearity will have contributions from excited-state absorption involving real excited states. We could also measure a small contribution from thermal scattering in the present case. Hence, it is appropriate to consider the observed nonlinearity as an effective three-photon process, where both genuine 3PA and sequential three-photon absorption contribute to the phenomenon.

3. Conclusion

We have investigated the structural, nonlinear optical, and magnetic properties of V_2O_5 nanoflowers synthesized by a novel low-temperature approach by means of XRD, TEM, EDAX, Raman, XPS, VSM, and Z-scan. We have observed room temperature ferromagnetism in the case of V_2O_5 flower structures for the first time. The ferromagnetic ordering is possible because of oxygen vacancies in the flower structures, as had been proposed recently[21,22] on the basis of theoretical calculations. The observation of its room temperature ferromagnetism suggests possible application of V_2O_5 flowers in spintronics. The nanoflowers are also shown to exhibit large nonlinear optical absorption leading to optical limiting, the main contribution being an effective three-photon absorption. In summary, V_2O_5 nanoflowers appear to be interesting nanosystems from the point of view of physical mechanisms operative in these materials as well as their potential in a variety of applications.

4. Experimental Section

The nanoflowers were characterized with a field-emission scanning electron microscope (HRSEM) using an FEI quanta FEG 200, as well as a transmission electron microscope (JEOL JEM 3010), X-ray diffraction (X'Pert PRO, diffractometer), and micro-Raman spectroscopy (LABRAMAN-HR) using a He−Ne laser (632.81 nm) in the backscattering geometry. The composition of the nanowires were analyzed with an energy-dispersive X-ray spectrometer (EDAX) attached to the FESEM. Magnetic measurements are performed by a vibrating magnetometer (LakeShore 7410 VSM system). Z-scan experiment is performed with a nanosecond Nd:YAG laser (Minilite, Continuum).

Acknowledgment. We thank the Department of Science and Technology Unit on Nanoscience, IIT Madras, for HRTEM and

XPS measurement and Defense Research and Development Organization, Government of India for funding.

References and Notes

(1) (a) Wang, Y.; Cao, G. *Chem. Mater.* **2006**, *18*, 2787. (b) Wang, Y.; Takahashi, K.; Lee, K.; Cao, G. *Adv. Funct. Mater.* **2006**, *16*, 1133. (c) Chernova, N. A.; Roppolo, M.; Dillon, A. C.; Whittingham, M. S. *J. Mater. Chem.* **2009**, *19*, 2526. (d) Xiong, C.; Aliev, A. E.; Gnade, B.; Balkus, K. J. *ACS Nano* **2008**, *2*, 293. (e) Li, B.; Xu, Y.; Rong, G.; Jing, M.; Xie, Y. *Nanotechnology* **2006**, *17*, 2560.

(2) (a) Kim, G. T.; Muster, J.; Krstic, V.; Park, J. C.; Roth, S.; Burghard, M. *Appl. Phys. Lett.* **2000**, *76*, 1875. (b) Myung, S.; Lee, M.; Kim, G. T.; Ha, J. S.; Hong, S. *Adv. Mater.* **2005**, *17*, 2361. (c) Muster, J.; Kim, G. T.; Krstic, V.; Park, J. G.; Park, Y. W.; Roth, S.; Burghard, M. *Adv. Mater.* **2000**, *12*, 420.

(3) Liu, J.; Wang, X.; Peng, Q.; Li, Y. *Adv. Mater.* **2005**, *17*, 764.

(4) (a) Chan, C. K.; Peng, H.; Twesten, R. D.; Jarausch, K.; Zhang, X. F.; Cui, Y. *Nano Lett.* **2007**, *7*, 490. (b) Hu, Y. S.; Liu, X.; Muller, J. O.; Schlogl, R.; Maier, J.; Su, D. S. *Angew. Chem., Int. Ed.* **2009**, *48*, 210. (c) Sides, C. R.; Martins, C. R. *Adv. Mater.* **2005**, *17*, 125. (d) Ragupathy, P.; Shivakumara, S.; Vasan, H. N.; Munichandraiah, N. *J. Phys. Chem. C* **2008**, *112*, 16700. (e) Ergang, N. S.; Lytle, J. C.; Lee, K. T.; Oh, S. M.; Smyrl, W. H.; Stein, A. *Adv. Mater.* **2006**, *18*, 1750. (f) Morcrette, M.; Rozier, P.; Dupont, L.; Mugnier, E.; Sannier, L.; Galy, J.; Tarascon, J. M. *Nat. Mater.* **2003**, *2*, 755.

(5) (a) Lee, H. Y.; Goodenough, J. B. *J. Solid State Chem.* **1999**, *148*, 81. (b) Kim, J. H.; Cho, B. W.; Lee, Y. H.; Kim, K. B. *J. Electrochem. Soc. A* **2006**, *153*, A1451.

(6) Yan, B.; Liao, L.; You, Y.; Xu, X.; Zheng, Z.; Shen, Z.; Ma, J.; Tong, L.; Yu, T. *Adv. Mater.* **2009**, *21*, 1.

(7) Gu, G.; Schmid, M.; Chiu, P. W.; Minett, A.; Fraysse, J.; Kim, G. T.; Roth, S.; Kozlov, M.; Munoz, E.; Baughman, R. H. *Nat. Mater.* **2003**, *2*, 316.

(8) Shao, M. W.; Lu, L.; Wang, H.; Wang, S.; Zhang, M. L.; Ma, D. D.; Lee, S. T. *Chem. Commun.* **2008**, *20*, 2310.

(9) (a) Díaz, G. C.; Piqueras, J. *J. Appl. Phys.* **2007**, *102*, 084307. (b) Díaz, G. C.; Piqueras, J. J. *Cryst. Growth Design* **2008**, *8*, 1031.

(10) (a) Zhou, L.; Mai, Y.; Liu, Y.; Qi, Y.; Dai, W.; Chen, *J. Phys. Chem. C* **2007**, *111*, 8202. (b) Chen, W.; Zhou, C.; Mai, L.; Liu, Y.; Qi, Y.; Dai, Y. *J. Phys. Chem. C* **2008**, *112*, 2262.

(11) Krusin-Elbaum, L.; Newns, D. M.; Zeng, H.; Derycke, V.; Sun, J. Z.; Sandstrom, R. *Nature* **2004**, *431*, 672.

(12) (a) Xu, J. F.; Czerw, R.; Webster, S.; Carroll, D. L. *Appl. Phys. Lett.* **2002**, *81*, 1711. (b) Hashimoto, T.; Yoko, T. *Appl. Opt.* **1995**, *34*, 2941.

(13) Teramura, K.; Tanaka, T.; Kani, M.; Hosokawa, T.; Funabiki, T. *J. Mol. Catal. A* **2004**, *208*, 299.

(14) (a) Dietl, T.; Ohono, H.; Matsukar, F.; Cibert, J.; Ferrand, D. *Science* **2000**, *287*, 1019. (b) Matsumoto, Y.; Murakami, M.; Shono, T.; Hasegawa, T.; Fukumura, T.; Kawasaki, M.; Ahmet, P.; Chikyow, T.; Koshihara, S.; Koinuma, H. *Science* **2001**, *291*, 854. (c) Sharma, P.; Gupta, A.; Rao, K. V.; Owens, F. J.; Sharma, R.; Ahuja, R.; Guillen, J. M. O.; Johansson, B.; Gehring, G. A. *Nat. Mater.* **2003**, *2*, 673.

(15) Ragupathy, P.; Shivakumar, S.; Vasan, S. H.; Munichandraiah, N. *J. Phys. Chem. C* **2008**, *112*, 16700.

(16) Baddour-Hudjean, R.; Pereira-Ramos, J. P.; Navone, N.; Smirnov, M. *Chem. Mater.* **2008**, *20*, 1916.

(17) Velazquez, J. M.; Banerjee, S. *Small* **2009**, *5*, 1025.

(18) (a) Wei, M.; Sugihara, H.; Honma, I.; Ichihara, M.; Zhou, H. *Adv. Mater.* **2005**, *17*, 2964. (b) Zhang, S.; Li, W.; Li, C.; Chen, J. *J. Phys. Chem. B* **2005**, *110*, 24855.

(19) Kosuge, K.; Takada, T.; Kachi, S. *J. Phys. Soc. Jpn.* **1963**, *18*, 318.

(20) (a) Gao, D.; Zhang, Z.; Fu, J.; Xu, Y.; Qi, J.; Xue, D. *J. Appl. Phys.* **2009**, *105*, 113928. (b) Kim, D.; Hong, J.; Park, Y. R.; Kim, K. J. *J. Phys.: Condens. Matter* **2009**, *21*, 195405. (c) Keating, P. R. L.; Scanlon, D. O.; Watson, G. W. *J. Phys.: Condens. Matter* **2009**, *21*, 405502. (d) Madhu, C.; Sundaresan, A.; Rao, C. N. R. *Phys. Rev. B* **2008**, *77*, 201306. (e) Sundaresan, A.; Bhargavi, R.; Rangarajan, N.; Siddesh, U.; Rao, C. N. R. *Phys. Rev. B* **2008**, *74*, 161306.

(21) Xiao, Z. R.; Guo, G. Y.; Lee, P. H.; Hsu, H. S.; Huang, J. C. A. *J. Phys. Soc. Jpn.* **2008**, *77*, 023706.

(22) Coey, J. M. D.; Venkatesan, M.; Fitzgerald, C. B. *Nat. Mater.* **2005**, *4*, 173.

(23) Tutt, L. W.; Boggess, T. F. *Prog. Quant. Electron.* **1993**, *17*, 299.

(24) Sheik-Behae, M.; Said, A. A.; Wei, T. M.; Hagan, D. J.; Stryland, E. W. V. *IEEE J. Quantum Electron.* **1990**, *26*, 760.

(25) Banfi, G. P.; Degiorgio, V.; Ricard, D. *Adv. Phys.* **1998**, *47*, 447.

(26) Suchand Sandeep, C. S.; Philip, R.; Satheeshkumar, R.; Kumar, V. *Appl. Phys. Lett.* **2006**, *89*, 063102.

(27) Banin, U.; Lee, C. J.; Guzelian, A. A.; Kadavanich, A. V.; Alivisatos, A. P.; Jaskolski, W.; Bryant, G. W.; Rosen, M. *J. Chem. Phys.* **1998**, *109*, 2306.

(28) Bawendi, M. G.; Wilson, W. L.; Rothberg, L.; Carroll, P. J.; Jedju, T. M.; Steigerwald, M. L.; Brus, L. E. *Phys. Rev. Lett.* **1990**, *65*, 1623.

(29) Kavan, L.; Gratzel, M.; Gilbert, S. E.; Klemenz, C.; Scheel, H. J. *J. Am. Chem. Soc.* **1996**, *118*, 6716.

(30) Sutherland, R. L. *Handbook of Nonlinear Optics*; Dekker: New York, 1996.

(31) (a) Adarsh, K. V.; Sangunni, K. S.; Suchand Sandeep, C. S.; Philip, R.; Kokenyesi, S.; Takats, V. *J. Appl. Phys.* **2007**, *102*, 026102. (b) Karthikeyan, B.; Suchand Sandeep, C. S.; Philip, R.; Baesso, M. L. *J. Appl. Phys.* **2009**, *106*, 114304.

JP107862N